

Magnetic activity and orbital parameters of CC Com based on photometric data, LAMOST low- and medium-resolution spectra

Zhong-Zhong Zhu (朱仲忠)¹, Li-Yun Zhang (张立云)^{2*}, Gang Meng (孟刚)^{2,3}, Yao Cheng (程瑶)^{2,3}, Liu Long (龙柳)^{2,3}, Xianming L. Han (韩先明)^{3,4}, Qing-Feng Pi (皮青峰)⁵ and Lin-Yan Jiang (江林焱)^{2,3}

¹ College of Big Data and Information Engineering, Guizhou University, Guiyang 550025, China

² College of Physics, Guizhou University, Guiyang 550025, China; liy_zhang@hotmail.com

³ Guizhou Provincial Key Laboratory of Public Big Data, Guizhou University, Guiyang 550025, China

⁴ Dept. of Physics and Astronomy, Butler University, Indianapolis, IN 46208, USA

⁵ College of Medicine, Guizhou University of Traditional Chinese Medicine, Guiyang 550025, China

Received 2020 February 24; accepted 2020 September 30

Abstract In this paper, we present four sets of photometric *VRI* light curves, and several LAMOST low and medium resolution spectra of contact binary CC Com. We revised the orbital parameters by simultaneously combining with previously published radial velocity measurements using the Wilson-Devinney program. We used light curves at different observational times to obtain the starspot parameters. The values of the starspot radius are variable in short- and long-term scales, and their longitudes are stable. We updated the orbital period change of CC Com, and analyzed the periodic variation. The period of CC Com decreases at a rate of $4.66 (\pm 0.20) \times 10^{-11} \text{ d yr}^{-1}$, which may be due to mass transfer from the secondary component to the primary component. The oscillation of its orbital period with a period of 17.18(0.08) years and amplitude of 0.0018(1)d may be caused by the light time effect (LITE) via a third body of $0.06 M_{\odot}$ dwarf or magnetic activity cycle. Furthermore, we obtained one optical spectrum from the LAMOST survey, which gives the spectral type of CC Com as $K7 \pm 2V$. Strong emissions exist in the $H\alpha$, and Ca II H&K lines in the observed spectrum, indicating strong chromospheric activity on CC Com. In the 12 LAMOST medium-resolution spectra, the EWs of $H\alpha$ line are variable along the phase and time, which may be a plage or flare event.

Key words: binaries: magnetic activity — stars: eclipsing — stars: individual (CC Com)

1 INTRODUCTION

Photometric and spectroscopic observations of eclipsing binaries are important for studying their stellar orbital parameters and magnetic activities. Multi-band photometric monitoring indicates that some eclipsing binaries exhibit period variation. Possible causes of period variation are the mass transfer between two components, stellar wind, third body, and magnetic activity cycle (Coughlin et al. 2008; Qian et al. 2013; Christopoulou et al. 2011; Lee et al. 2016; Li et al. 2019). Light curve asymmetry (O’Connell effect) has been observed on many eclipsing binaries (O’Connell 1951). Therefore, we studied starspot activities of some binaries, known to be associated with light curve asymmetry, by performing long-term photometric observations. Furthermore, we studied their magnetic

activity by using the spectroscopic observations of the Balmer, and Ca II H&K lines (Zhang et al. 2018).

Active binaries are important for studying the magnetic activity phenomena and statistical properties. Pi et al. (2019) obtained starspot activity cycles of DV Psc based on approximately 10 years of photometric observations. In long-term photometric monitoring programs, astronomers have detected many flare events of active binaries and determined their corresponding flare parameters (amplitude, duration, etc) (Qian et al. 2012; Luo et al. 2019; Pi et al. 2019; Dal & Özdarcın 2018). Cao et al. (2019) determined chromospheric activity indicators, and detected plage, flare event and prominence. Şenavcı et al. (2018) determined the relationship between chromospheric plage and starspot region of SV Cam. We are performing follow-up observations of active eclipsing binaries using the Large Sky Area Multi-Object Fiber

* Corresponding author

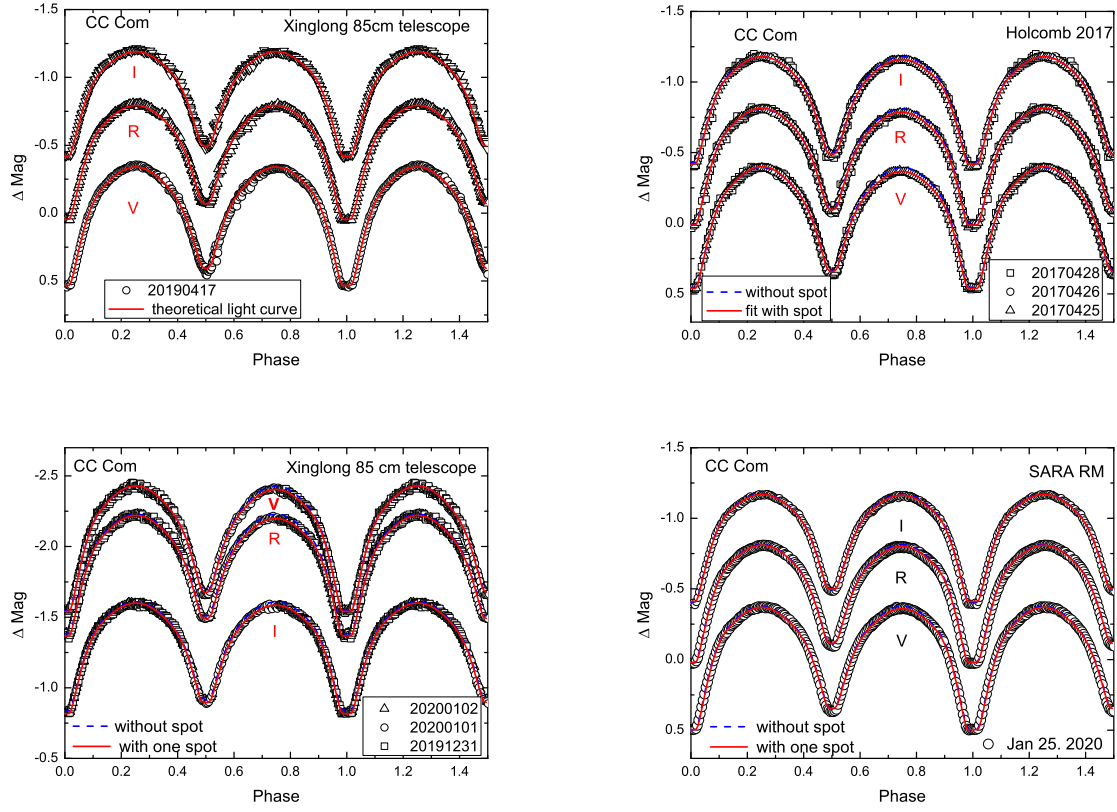


Fig. 1 Theoretical and observational light curves of CC Com.

Spectroscopic Telescope (LAMOST) spectral survey to study their magnetic properties.

CC Com has been identified as an eclipsing binary via two-color photometry (Zhukov 1976). Rucinski (1976) obtained its photometric orbital parameters (inclination, mass ratio, and contact factor) using simultaneous BV light curves. Klemola (1977) discussed the motions of CC Com and discovered that it is not a member of the Coma star cluster. The authors also obtained its absolute elements using light curves and radial velocities, and observed the emission peaks of Ca II H&K lines. Maceroni et al. (1982) determined similar absolute elements of CC Com using the Wilson and Devinney program (Wilson & Devinney 1971), but did not discuss the light curve asymmetry. Furthermore, different maximum values of the light curves were determined in different seasons (Zhukov 1983). McLean & Hilditch (1983) analyzed the radial velocity curves and derived a similar spectroscopic mass ratio. The long-term fluctuation of the light curve of CC Com may be due to the cool starspots on the surface of the primary component (Zhukov 1985). Bradstreet (1985) also explained light curves with starspots. Combined with the spectroscopic results of Rucinski (1976), Zhou (1988) estimated its absolute parameters using *UBV*

light curves. Pribulla et al. (2007) re-measured the radial velocities. Köse et al. (2011) determined more precise orbital parameters and summarized the most published orbital parameters of CC Com. CC Com was in the contact configuration based on a model from multi-color light curves (Zola et al. 2010).

The orbital period of CC Com has been studied by the several authors (Qian 2001; Yang & Liu 2003; Yang et al. 2009; Köse et al. 2011). It was demonstrated that its period exhibited a secular decrease with superimposed oscillation (Qian 2001). Its period showed a secular decrease at a rate of $2 \times 10^{-8} \text{ d yr}^{-1}$ (Yang & Liu 2003). Yang & Liu (2003) also found an oscillation with a periodicity of 16.1 years. However, Yang et al. (2009) revised the period and amplitude of cyclic variation as 23.6(0.4) yr and $A = 0.0028(3) \text{ d}$. The cycle of short-term oscillations may be explained by a magnetic activity cycle or a third body (Yang et al. 2009).

In this work, we present new photometric data and LAMOST spectra for CC Com. We used the Wilson-Devinney program (Wilson 1979, 1990, 1994, 2008) to revise the orbital parameters. Furthermore, we discuss its period variation, and determine chromospheric

Table 1 Observational Log of CC Com, Comparison and Check Stars

Target	Name	Coordinate(RA;Dec 2000)	Mag _{-J}	Mag _{-H}	Mag _{-K}	Source
Variable star	CC Com	12:12:06.04;+22:31:58.7	8.986	8.341	8.245	[1]
Comparison star1	2MASS J12114530+2239030	12:11:45.35;+22:39:02.7	10.572	10.274	10.228	[1]
Comparison star2	2MASS J12120505+2230569	12:12:05.21;+22:30:56.3	10.273	9.668	9.419	[1]
Check star	2MASS J12114222+2235131	12:11:42.24;+22:35:12.9	12.179	11.782	11.784	[1]

[1] Cutri et al. (2003); The J , H and K magnitudes are from 2Mass survey.

Table 2 New VRI Light Curve Data of CC Com

V Band		R Band		I Band		Telescope
HJD(+2400000)	Δ mag	HJD(+2400000)	Δ mag	HJD(+2400000)	Δ mag	
57868.62375	0.230	57868.62409	-0.229	57868.62438	-0.653	Holcomb telescope
57868.62473	0.191	57868.62507	-0.266	57868.62535	-0.686	Holcomb telescope
57868.62570	0.153	57868.62604	-0.301	57868.62632	-0.715	Holcomb telescope
58590.99775	-0.206	58590.99797	-0.661	58590.99815	-1.049	Xinglong 85 telescope
58591.00543	-0.090	58591.00566	-0.555	58591.00584	-0.967	Xinglong 85 telescope
58591.00652	-0.058	58591.00675	-0.554	58591.00691	-0.925	Xinglong 85 telescope
58849.28544	-2.403	58849.28556	-2.187	58849.28568	-1.588	Xinglong 85 telescope
58849.28606	-2.405	58849.28619	-2.175	58849.28630	-1.583	Xinglong 85 telescope
58849.28667	-2.402	58849.28681	-2.187	58849.28693	-1.570	Xinglong 85 telescope
58873.53431	-0.237	58873.53455	-0.684	58873.53475	-1.045	SARA RM telescope
58873.53545	-0.257	58873.53568	-0.699	58873.53589	-1.055	SARA RM telescope
58873.53659	-0.267	58873.53682	-0.702	58873.53702	-1.078	SARA RM telescope
...

This full table is available in <http://www.raa-journal.org/docs/Supp/ms4752Table2.dat>.

activity using the low- and medium-resolution spectra of LAMOST (Zhang et al. 2020).

2 PHOTOMETRIC AND SPECTROSCOPIC OBSERVATIONS

2.1 Photometric Observations

We conducted four new sets of observations. The first was performed on 2019 April 17, and the second on 2019 December 31 and 2020 January 1 and 2. Both the first and second sets were conducted using the 85 telescope at the National Astronomical Observatories of China (NAOC). The camera used was a 1024×1024 pixel CCD and the filter was the Johnson-Cousin-Bessell $BVRI$ system (Zhou et al. 2009). The third set was performed in the VRI bands using the Holcomb Telescope on 2017 April 25, 26, and 28, with a field of view of approximate $18' \times 18'$. The fourth set was obtained on 2020 January 25 using the SARA RM 1.0 telescope with a $11.6' \times 11.6'$ field of view (Keel et al. 2017). All four datasets were processed with IRAF¹, including standard bias, flat-field, and cosmic-ray removal corrections, as well as standard aperture photometry for the binary, comparison, and check stars. Their parameters are listed in Table 1. The light curves of the CC Com are shown in Figure 1. All photometric data are listed in Table 2.

¹ IRAF (<http://iraf.noao.edu/>) is distributed by the National Optical Astronomy Observatories, which are operated by the Association of Universities for Research in Astronomy, Inc., under cooperative agreement with the National Science Foundation.

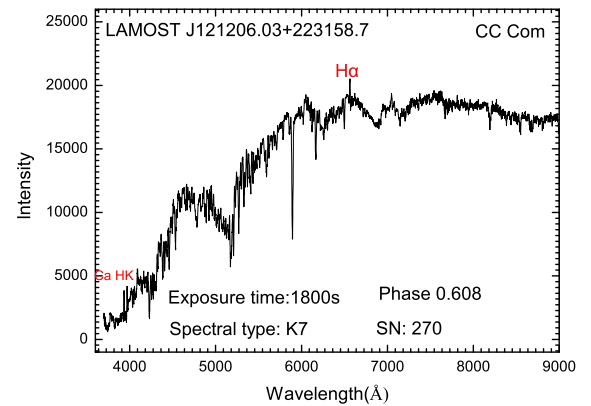


Fig. 2 LAMOST low-resolution spectrum of CC Com.

2.2 LAMOST Spectral Observations

LAMOST is a 4 m Schmidt optical telescope for spectral survey (Cui et al. 2012). LAMOST spectra are useful for studying the spectral properties and magnetic activities of eclipsing binaries (Zhang et al. 2018). By cross-matching CC Com with LAMOST DR6², we obtained one LAMOST spectrum with a resolution of $R \sim 1800$ and a signal to noise ratio (SN) of approximate 271 on 2013 December 21. The parameters for CC Com are the time of the spectrum observation (HJD:2456647.9125), spectral type ($K7 \pm 2$), exposure time of the spectrum (1800s),

² <http://dr6.lamost.org/>

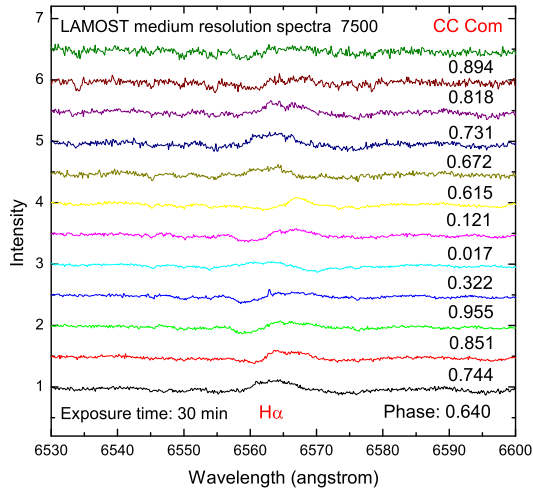


Fig. 3 LAMOST medium-resolution $H\alpha$ lines of CC Com.

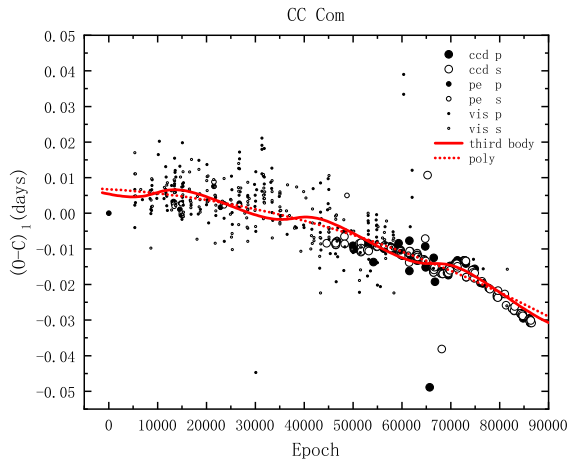


Fig. 4 Period variation of CC Com. *Dashed line* represents parabolic fit, and *solid line* represents the fit of a third body.

stellar effective temperature ($4148 (\pm 39)\text{K}$), and stellar surface gravity ($\log g 4.485 \pm 0.064$) (Luo et al. 2015). The fundamental parameters were obtained by fitting the model and observation spectrum (Wu et al. 2011). Emissions of the $H\alpha$ and Ca II H&K lines were observed, as shown in Figure 2. LAMOST medium-resolution ($R \sim 7500$) spectral survey began in September 2017. The wavelength range of the blue arm is $4950 \sim 5350 \text{ \AA}$ and that of the red region is $6300 \sim 6800 \text{ \AA}$ (Liu et al. 2019, 2020). We are interested in the red region because of the $H\alpha$ line, which can be used to discuss chromospheric activity (Zhang et al. 2020). Therefore, we searched for CC Com from the LAMOST database and obtained 12 medium-resolution spectra from observations performed on 2018

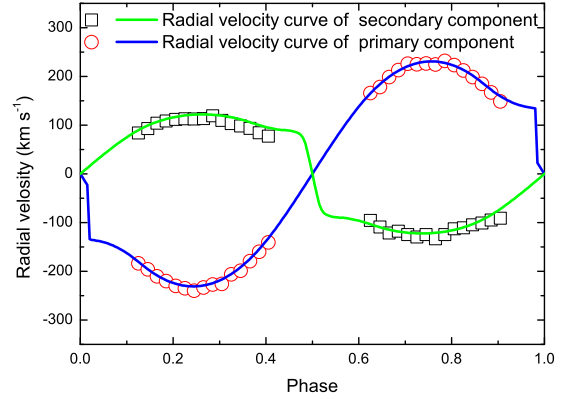


Fig. 5 Theoretical and observational radial velocity curves of CC Com.

April 25, May 7, 24, 25, and June 2. We listed the LAMOST medium-resolution observational log in Table 3, which includes the observational date, exposure time, HJD, phase, SN, and the equivalent widths (EWs) and height in the $H\alpha$ line. All these LAMOST medium-resolution spectra are shown in Figure 3. There are obvious strong emissions of the $H\alpha$ line in the orbital phases 0.640, 0.672, 0.731 and 0.818. However, there are some absorption components in the profile of $H\alpha$ line in the orbital eclipse phases 0.017 and 0.955. This might be caused by the effect of the eclipses.

3 PERIOD ANALYSIS

We fitted the light curve of each band using the method described by Kwee & van Woerden (1956), and obtained six new light minimum times. We listed them in Table 4. To obtain a revised ephemeris, we collected all the minimum times of CC Com from O-C Gateway³ and other literature. We collected 574 data points, and listed the light minimum times, uncertainties, types of light minimum time, observation methods, and corresponding references in Table 4. These 574 data points included 28 photoelectric data points, 350 visual data points and 196 CCD data points. By analyzing these 580 data points (574 from the literature and six new ones from this study), we obtained a revised linear ephemeris for CC Com.

$$\text{Min.}I = \text{HJD}2439533.5959 (\pm 0.0007) + 0^{\text{d}}.2206859 (\pm 0.0000001)E. \quad (1)$$

We calculated the number of cycles (epoch) of CC Com and the corresponding residuals $((O-C)I)$, which are listed in Table 4 using this new ephemeris. During fitting for Equation (1), we assigned different weighting factors to the

³ <http://var2.astro.cz/>, <https://www.aavso.org/>

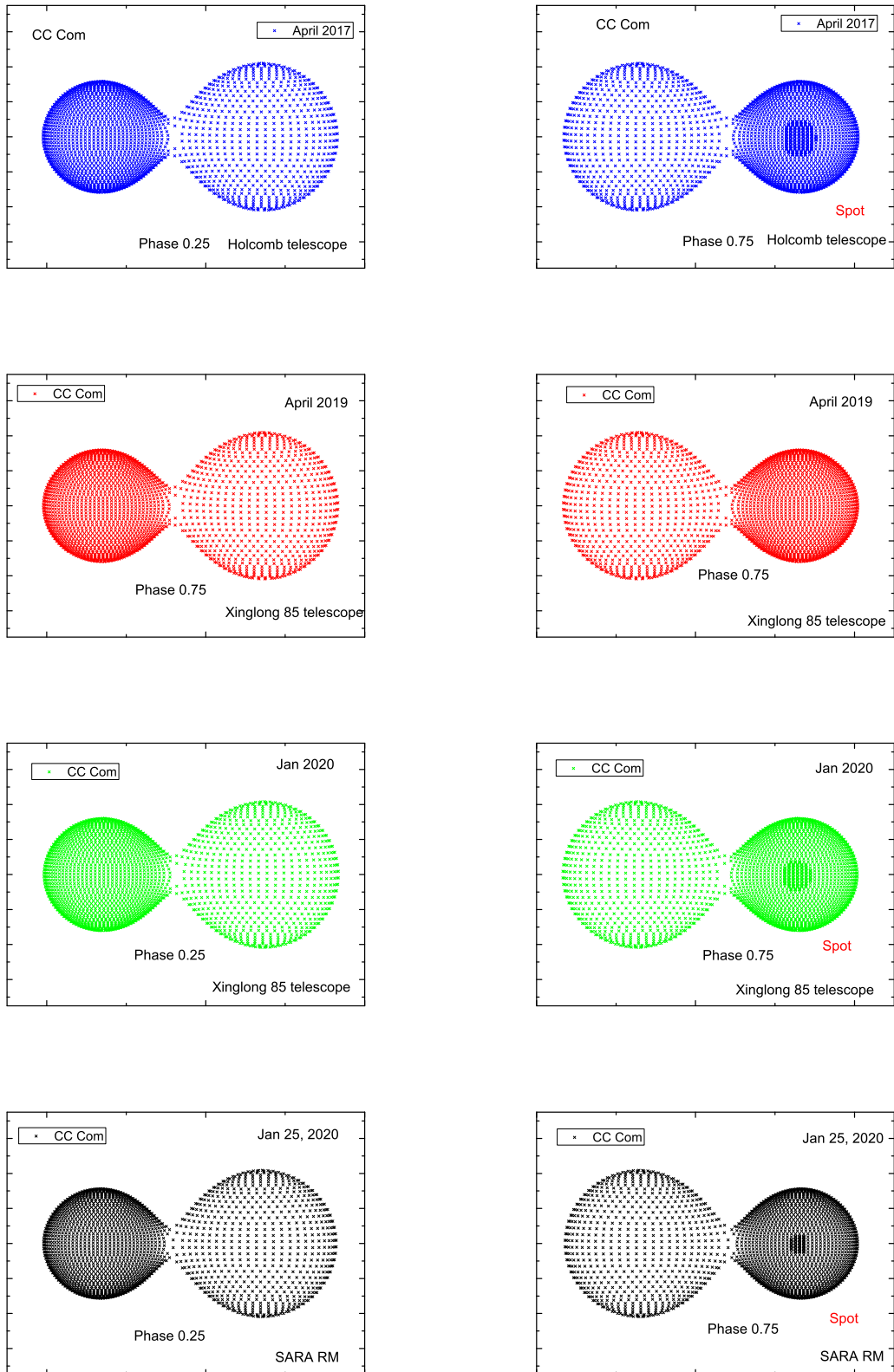


Fig. 6 Starspot configurations of CC Com in different time.

Table 3 Log of LAMOST Medium Spectroscopic Survey of CC Com, and Intensity and Height of H α Line

Date	HJD(2400000+) (d)	Exposure time (s)	SN	Phase	EW H α (Å)	Height H α (Å)
2018-04-25	58233.54792	1800	134	0.64047	-0.1625 ± 0.0184	1.046 ± 0.010
2018-04-25	58233.57083	1800	134	0.74432	-0.1882 ± 0.0877	1.123 ± 0.004
2018-04-25	58233.59444	1800	134	0.85131	-0.3224 ± 0.0707	1.091 ± 0.011
2018-04-25	58233.61736	1800	134	0.95515	-0.3037 ± 0.0347	1.076 ± 0.015
2018-05-07	58245.61528	1800	108	0.32163	-0.3870 ± 0.0167	1.039 ± 0.005
2018-05-24	58262.54097	1800	101	0.01749	-0.3541 ± 0.0496	1.080 ± 0.011
2018-05-24	58262.56389	1800	101	0.12134	$+0.2546 \pm 0.0841$	1.094 ± 0.007
2018-05-25	58263.55556	1800	54	0.6149	$+0.5166 \pm 0.0506$	1.084 ± 0.009
2018-05-25	58263.56806	1800	54	0.67154	$+0.8837 \pm 0.0132$	1.152 ± 0.008
2018-05-25	58263.58125	1800	54	0.73133	$+0.7315 \pm 0.0046$	1.114 ± 0.002
2018-06-02	58271.54514	1800	35	0.81832	-0.0721 ± 0.0660	1.031 ± 0.031
2018-06-02	58271.56181	1800	35	0.89384	-0.5446 ± 0.0918	1.008 ± 0.010

Table 4 Minimum Times and Relevant Parameters of CC Com

JD(Hel.)	Error	Min	Method	Cycle	(O-C) ₁	(O-C) ₂ (3rd body)	Reference
2440711.3880	0.0020	p	vis	5337.0	0.0046	-0.00231	[1]
2440711.5130	0.0020	s	vis	5337.5	0.0192	0.01239	[1]
...	...	p
2457839.3723	0.0002	s	CCD	82949.5	0.0076	-0.00234	[47]
2458591.0270	0.0016	s	CCD	86355.5	0.0062	-0.00211	[48]
2458591.1370	0.0001	p	CCD	86356.0	0.0059	-0.00241	[48]
2458591.2492	0.0021	s	CCD	86356.5	0.0077	-0.00051	[48]
2457869.6067	0.0005	S	CCD	83086.5	0.0080	-0.00182	[48]
2457868.7247	0.0009	s	CCD	83082.5	0.0087	-0.00112	[48]
2457871.7030	0.0008	P	CCD	83096.0	0.0078	-0.00201	[48]
2457871.8134	0.0022	S	CCD	83096.5	0.0078	-0.00201	[48]
2458849.3378	0.0004	P	CCD	87526.0	0.0042	-0.00355	[48]
2458850.3308	0.0001	P	CCD	87530.5	0.0041	-0.00365	[48]
2458851.3249	0.0006	P	CCD	87535.0	0.0051	-0.00265	[48]
2458851.4347	0.0006	S	CCD	87535.5	0.0046	-0.00325	[48]

[1] Paschke & Brat (2006); [2] Zhukov (1983); [3] Ogoza (1995); [4] Agerer & Hubscher (1996); [5] Ogloza (1997); [6] Agerer & Huebscher (1997); [7] Agerer & Huebscher (1998); [8] Safar & Zejda (2000); [9] Agerer & Hubscher (1999); [10] Yang & Liu (2003); [11] Ogloza et al. (2000); [12] Agerer & Hubscher (2000); [13] Safar & Zejda (2002); [14] Agerer & Hubscher (2002); [15] Kim et al. (2004); [16] Nelson (2004); [17] Agerer & Hubscher (2003); [18] Kim et al. (2006); [19] Hubscher et al. (2005); [20] Hubscher (2005); [21] Hubscher et al. (2006); [22] Pribulla et al. (2005); [23] Nelson (2006); [24] Hubscher (2007); [25] Hubscher et al. (2006); [26] Parimucha et al. (2007); [27] Dogru et al. (2007); [28] Parimucha et al. (2007); [29] Borkovits et al. (2008); [30] Dogru et al. (2007); [31] Nelson (2009); [32] Hubscher et al. (2009); [33] Dvorak (2009); [34] Diethelm (2009); [35] Hubscher et al. (2010); [36] Parimucha et al. (2011); [37] Diethelm (2010); [38] Hubscher et al. (2012); [39] Diethelm (2011); [40] Parimucha et al. (2013); [41] Nelson (2013); [42] Hubscher & Lehmann (2013); [43] Bahar et al. (2017); [44] Parimucha et al. (2007); [45] Basturk et al. (2014); [46] Nelson (2016); [47] Pagel (2018); [48] our paper.

This full table is available in <http://www.raa-journal.org/docs/Supp/ms4752Table4.dat>.

data with different observation methods. For example, the weights of visual and photographic data were assigned to 1, and the weights of the photoelectric and CCD data were assigned to 10. Figure 4 shows (O-C)₁ versus the epoch. We can see that the period variation of CC Com exhibits a downward parabolic trend with a weak oscillation. Therefore, we fitted them by the parabolic function and light time effect (LITE) (Yang et al. 2007), as shown in Figure 4, and obtained the ephemeris:

$$\begin{aligned} \text{Min.}I &= \text{HJD}2439531.0733(\pm 0.0005) \\ &+ 0^{\text{d}}.2206862(\pm 0.0000001)E \\ &- 0.141(\pm 0.006) \times 10^{-13}E^2 + \tau. \end{aligned} \quad (2)$$

$$\tau = \frac{a_{12} \sin i'}{c} \left(\frac{1 - e'^2}{1 + e' \cos \nu'} + e' \sin \omega' \right). \quad (3)$$

The parabolic fit and fitting result of the LITE are indicated by the dashed and red lines, respectively. The quadratic term of Equation (2) is $-0.141(\pm 0.006) \times 10^{-13}$, which means that the orbital period decreases at a rate of $dP/dt = 4.66 (\pm 0.20) \times 10^{-11} \text{ d yr}^{-1}$. In Equations (2) and (3), $A = a_{12} \sin i'/c$ is the semi-amplitude of the LITE, a_{12} is the semi-axis of the eclipsing-pair orbit around the common center of mass with the third body, and c represents the speed of light. These parameters were calculated using the Levenberg-Marquardt technique (Press et al. 1992; Yang et al. 2011), and the results are shown in Table 5. The oscillation with 17.18 ± 0.08 years may be explained by the LITE via a third body. If we assumed that the orbital inclination was 90 degree, then the minimum mass of the third body would be approximate $0.06 M_{\odot}$, which might imply a dwarf with spectral type

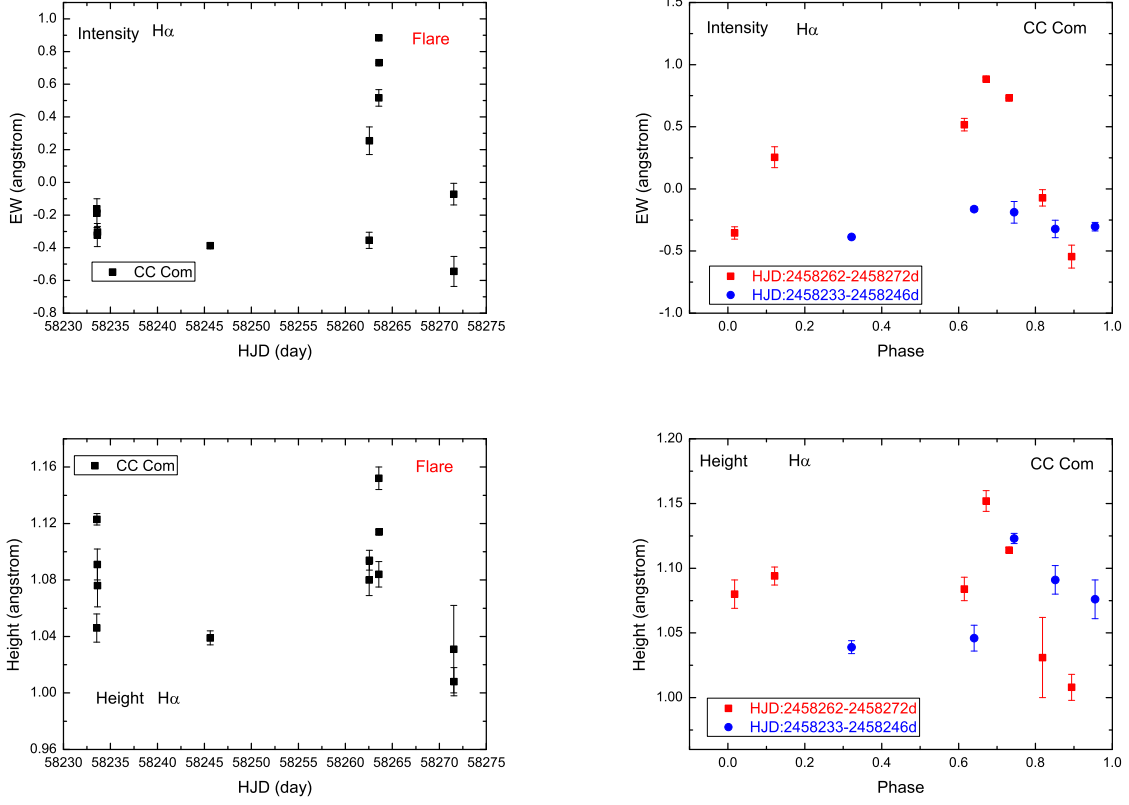


Fig. 7 EW (*top*) and height (*bottom*) of $H\alpha$ line of CC Com vs HJD (*left*) and orbital phase (*right*).

Table 5 Third Body Parameters of CC Com

Parameter	Value
A (d)	$0.0018(\pm 0.0001)$
P_3 (yr)	$17.18(\pm 0.08)$
e	$0.32(\pm 0.03)$
T_0 (HJD)	2439533.5830
$a_{12} \sin i$ (AU)	$0.33(\pm 0.02)$
K_{RV} (km s^{-1})	$0.58(\pm 0.26)$
$f(m)$ (M_\odot)	$0.00013(\pm 0.00002)$

M7-M9 according to the relationship between spectral type and mass (Cox 2000). However, the fitting is poor for the variation of the orbital period shown in Figure 4 and is attributable to two possible reasons. One is that 61% of the light curve minimum data points of CC Com are visual data, which are inherently imprecise, unlike modern CCD data. Furthermore, the amplitude of the third body of CC Com is extremely low, because CC Com is a low mass eclipsing binary with $0.409 M_\odot$ and $0.748 M_\odot$ components. More accurate light curve minima are required to confirm the mechanism.

4 ORBITAL PARAMETERS

From our observations, we obtained four sets of multi-bands and full-phase photometric data, as shown in

Figure 1. We combined the radial velocity curves of Pribulla et al. (2007) and our new data to obtain absolute orbital parameters using the WD program. We selected Mode 3 (contact binary) and set the temperature of the primary component (T_1) to 4148K. The temperature was based on the LAMOST spectra, which is similar to the previous result of Köse et al. (2011). The bolometric albedo and gravity-darkening (g) coefficients were set to 0.5 and 0.32, respectively. Meanwhile, the bolometric and limb-darkening coefficients were determined using the following methods used in the previous papers (Ruciński 1973; van Hamme 1993). Among our four sets of light curves, we selected the symmetrical light curve of 2019 April 15 to obtain the orbital parameters, and listed the results of CC Com in Table 6. The corresponding radial velocity curve fitting results are plotted in Figure 5. Furthermore, we also plotted the corresponding theoretical light curves and the geometric configurations in Figures 1 and 6, respectively. To analyze other light curves of CC Com, we used the newly obtained orbital parameters to fit the light curves observed at other times. The O’Connell effect was observed in other three sets of light curves, where the light curves near the 0.25 phase were higher than those near the 0.75 phase. We added a cool spot near

Table 6 Parameter Values of CC Com Obtained from Four Sets of Observations

Parameter	April 2019	April 2017	Jan 1&2 2020	Jan 25 2020
T_1	4148 ± 40 K			
Bol1	0.474			
Bol2	0.341			
X_{1V}	0.757			
X_{2V}	0.618			
X_{1R}	0.644			
X_{2R}	0.556			
X_{1I}	0.509			
X_{2I}	0.420			
VGAM=SYSTEMIC RADIAL VELOCITY	-0.050 ± 0.039	-0.048 ± 0.030	-0.048 ± 0.049	-0.049 ± 0.016
a	1.61 ± 0.04	1.61 ± 0.03	1.61 ± 0.05	1.61 ± 0.02
$M_1(M_\odot)$	0.409	0.410	0.408	0.409
$M_2(M_\odot)$	0.748	0.749	0.746	0.748
$R_1(R_\odot)$	0.560	0.550	0.560	0.550
$R_2(R_\odot)$	0.730	0.720	0.730	0.720
T_2	3984 ± 3 K	3987 ± 2 K	3974 ± 1 K	3967 ± 1 K
$\Omega_1 = \Omega_2$	4.877 ± 0.008	4.887 ± 0.003	4.874 ± 0.002	4.915 ± 0.002
$i(^{\circ})$	87.4 ± 0.1	87.7 ± 0.1	89.0 ± 0.1	89.3 ± 0.1
$q(M_2/M_1)$	1.828 ± 0.006	1.828 ± 0.006	1.828 ± 0.006	1.828 ± 0.006
$L_{1V}/(L_{1V} + L_{2V})$	0.432 ± 0.002	0.431 ± 0.001	0.438 ± 0.001	0.439 ± 0.001
$L_{1R}/(L_{1R} + L_{2R})$	0.424 ± 0.001	0.422 ± 0.001	0.428 ± 0.001	0.430 ± 0.001
$L_{1I}/(L_{1I} + L_{2I})$	0.406 ± 0.001	0.405 ± 0.001	0.409 ± 0.001	0.409 ± 0.002
r_1 (Pole)	0.3189 ± 0.0009	0.3180 ± 0.0003	0.3192 ± 0.0002	0.3153 ± 0.0002
r_1 (Side)	0.3350 ± 0.0012	0.3338 ± 0.0004	0.3353 ± 0.0003	0.3306 ± 0.0002
r_1 (Back)	0.3756 ± 0.0020	0.3737 ± 0.0006	0.3761 ± 0.0004	0.3685 ± 0.0004
r_2 (Pole)	0.4184 ± 0.0008	0.4175 ± 0.0003	0.4187 ± 0.0002	0.4149 ± 0.0002
r_2 (Side)	0.4462 ± 0.0010	0.4450 ± 0.0004	0.4465 ± 0.0003	0.4417 ± 0.0003
r_2 (Back)	0.4797 ± 0.0015	0.4781 ± 0.0005	0.4802 ± 0.0004	0.4736 ± 0.0003
Lat_{s1}		90	90	90
$Long_{s1}$		269.8 ± 0.4	271.0 ± 0.3	270.8 ± 0.3
r_{s1}		18.3 ± 0.8	15.5 ± 0.3	10.8 ± 0.2
S_1 T		3733 ± 23	3733 ± 21	3733 ± 42
σ	0.364	0.445	1.984	0.089

the 0.75 phase on the primary component in the fitting (see right side in Fig. 6). As we could not obtain the spot latitudes because of the traditional light curve fitting, we assumed the spot latitude to be on the equator (90°). We listed the fitting parameters in the second to fourth columns of Table 6.

5 DISCUSSION

The new orbital parameters are similar to those obtain in previous studies (Rucinski 1976; Zhukov 1985; Zhou 1988; Zola et al. 2010; Köse et al. 2011). We obtained a contact factor of 21.8%, which is consistent with values obtained in the previous studies (Rucinski 1976; Köse et al. 2011). There is oscillation in the period change of CC Com, which is attributable to the third body of the 0.06 M_\odot dwarf or magnetic activity cycle (Applegate 1992; Applegate 1992) since CC Com exhibits strong magnetic activity. A decrease in the period will result in the shrinking of the critical Roche lobe. Consequently, the contact degree of CC Com will increase. The oscillation of the orbital period is similar to the result obtained by Yang & Liu (2003), but is smaller than that by Yang et al. (2009). More data are required to confirm this. Our four

sets of light curves, each from a different observation time, demonstrated light curve variations. With regard to the spot parameters, the spot temperature and radius exhibits a strong anti-correlation. The spot temperatures were similar in April 2017, December 2019, and January 2020 datasets. Long-term variations were observed for the spot radius. The light curve variability was similar to that of Zhukov (1983). The spot longitude obtained using this method is precise. The spot longitudes from different observation times were similar, which indicates that the spot position was stable in all years.

There are obvious emissions in the $H\alpha$ and Ca II H&K lines from LAMOST low-resolution spectrum in Figure 2. Because the spectrum was low-resolution, we could not distinguish the lines of the primary and secondary components. The LAMOST medium-resolution spectra had a higher resolution than the LAMOST low-resolution spectra. However, we could not distinguish the emission from the primary or secondary components of CC Com in the observed $H\alpha$ lines because CC Com had a high contact factor of approximate 21.8%. Therefore, we did not treat the individual component profile of CC Com. We calculated the EWs and uncertainties of the profile of both components in the $H\alpha$ line by integrating them over

the emission line. Furthermore, we obtained the height of the $H\alpha$ line. We listed the results in Table 3 and plotted them against HJD in Figure 7. The EW of $H\alpha$ line was consistent with its height. Long time scale variations were observed in the chromospheric activity. To reduce the effect of long-term variation on the chromospheric activity, we segregated our data into two parts in HJD: 2458262–2458272d and 2458233–2458246d. We plotted two sets of chromospheric activities with orbital phases, as shown in the right panel of Figure 7. There are orbital modulation variations of EWs of $H\alpha$ line. The EWs around phase 0.75 (non-eclipse phase) is higher than that of orbital phase 0 (eclipsing phase). There are two reasons to explain that. One reason is a plage or flare event around phase 0.75. The other is the effect of the eclipses. The region of chromospheric activity of CC Com was consistent with its photospheric starspots from the light curves, both were at similar orbital phases. More photometric and spectroscopic observations are required to determine the relationship between the photospheric starspots and chromospheric activity.

6 CONCLUSIONS

The analysis on photometric and spectroscopic observations of CC Com performed in this study can be summarized as follows:

1. We revised the absolute orbital parameters based on our new light curves and published radial velocities. The values of the starspot radius were variable, and their longitudes were stable.
2. We confirmed that CC Com underwent a continuous period decrease overlaid with a periodic oscillation.
3. Strong emissions were observed in the $H\alpha$ and Ca II H&K lines of the LAMOST low-resolution spectrum, indicating strong chromospheric activities.
4. Based on the LAMOST medium-resolution spectra of CC Com, there are variabilities in EWs of $H\alpha$ lines along the orbital phases and time.

Acknowledgements Our research was supported by the Joint Research Fund in Astronomy (Nos. 11963002 and U1631236) under a cooperative agreement between NSFC and CAS. We acknowledge the support of the staff of the Xinglong 85 cm telescope and Cultivation Project for LAMOST Scientific Payoff and Research Achievement of CAMS-CAS.

References

- Agerer, F., & Hubscher, J. 1996, *Information Bulletin on Variable Stars*, 4383, 1

- Agerer, F., & Huebscher, J. 1997, *Information Bulletin on Variable Stars*, 4472, 1
- Agerer, F., & Huebscher, J. 1998, *Information Bulletin on Variable Stars*, 4606, 1
- Agerer, F., & Hubscher, J. 1999, *Information Bulletin on Variable Stars*, 4711, 1
- Agerer, F., & Hubscher, J. 2000, *Information Bulletin on Variable Stars*, 4912, 1
- Agerer, F., & Hubscher, J. 2002, *Information Bulletin on Variable Stars*, 5296, 1
- Agerer, F., & Hubscher, J. 2003, *Information Bulletin on Variable Stars*, 5484, 1
- Applegate, J. H. 1992, *ApJ*, 385, 621
- Bahar, E., Yorukoglu, O., Esmer, E. M., et al. 2017, *Information Bulletin on Variable Stars*, 6209, 1
- Basturk, O., Bahar, E., Senavci, H. V., et al. 2014, *Information Bulletin on Variable Stars*, 6125, 1
- Borkovits, T., van Cauteren, P., Lampens, P., et al. 2008, *Information Bulletin on Variable Stars*, 5835, 1
- Bradstreet, D. H. 1985, *ApJS*, 58, 413
- Cao, D., Gu, S., Ge, J., et al. 2019, *MNRAS*, 482, 988
- Christopoulou, P.-E., Parageorgiou, A., & Chrysopoulos, I. 2011, *AJ*, 142, 99
- Coughlin, J. L., Dale, H. A., & Williamon, R. M. 2008, *AJ*, 136, 1089
- Cox, A. N., 2000, *Allen's Astrophysical Quantities*. Springer, New York, P. 388
- Cui, X.-Q., Zhao, Y.-H., Chu, Y.-Q., et al. 2012, *Research in Astronomy and Astrophysics*, 12, 1197
- Cutri, R. M., Skrutskie, M. F., van Dyk, S., et al. 2003, *VizieR Online Data Catalog*, II/246
- Dal, H. A., & Özdarcan, O. 2018, *MNRAS*, 474, 326
- Diethelm, R. 2009, *Information Bulletin on Variable Stars*, 5894, 1
- Diethelm, R. 2010, *Information Bulletin on Variable Stars*, 5945, 1
- Diethelm, R. 2011, *Information Bulletin on Variable Stars*, 5992, 1
- Dogru, S. S., Dogru, D., Erdem, A., et al. 2006, *Information Bulletin on Variable Stars*, 5707, 1
- Dogru, S. S., Dogru, D., & Donmez, A. 2007, *Information Bulletin on Variable Stars*, 5795, 1
- Dvorak, S. W. 2009, *Information Bulletin on Variable Stars*, 5870, 1
- Hubscher, J. 2005, *Information Bulletin on Variable Stars*, 5643, 1
- Hubscher, J., Paschke, A., & Walter, F. 2005, *Information Bulletin on Variable Stars*, 5657, 1
- Hubscher, J., Paschke, A., & Walter, F. 2006, *Information Bulletin on Variable Stars*, 5731, 1
- Hubscher, J. 2007, *Information Bulletin on Variable Stars*, 5802, 1

- Hubscher, J., Steinbach, H.-M., & Walter, F. 2009, *Information Bulletin on Variable Stars*, 5874, 1
- Hubscher, J., Lehmann, P. B., Monninger, G., et al. 2010, *Information Bulletin on Variable Stars*, 5918, 1
- Hubscher, J., Lehmann, P. B., & Walter, F. 2012, *Information Bulletin on Variable Stars*, 6010, 1
- Hubscher, J. & Lehmann, P. B. 2013, *Information Bulletin on Variable Stars*, 6070, 1
- Keel, W. C., Oswalt, T., Mack, P., et al. 2017, *PASP*, 129, 015002
- Kim, S.-L., Kang, Y. B., Koo, J.-R., et al. 2004, *Information Bulletin on Variable Stars*, 5538, 1
- Kim, C.-H., Lee, C.-U., Yoon, Y.-N., et al. 2006, *Information Bulletin on Variable Stars*, 5694, 1
- Klemola, A. R. 1977, *PASP*, 89, 402
- Köse, O., Kalomeni, B., Keskin, V., et al. 2011, *Astronomische Nachrichten*, 332, 626.
- Kwee, K. K. & van Woerden, H. 1956, *Bull. Astron. Inst. Netherlands*, 12, 327
- Lee, J. W., Hong, K., Koo, J.-R., et al. 2016, *ApJ*, 820, 1
- Li, K., Xia, Q.-Q., Liu, J.-Z., et al. 2019, *RAA (Research in Astronomy and Astrophysics)*, 19, 147
- Liu, C., Fu, J., Shi, J., et al. 2020, arXiv e-prints, arXiv:2005.07210
- Liu, N., Fu, J.-N., Zong, W., et al. 2019, *RAA (Research in Astronomy and Astrophysics)*, 19, 075
- Luo, C., Zhang, X., Wang, K., et al. 2019, *ApJ*, 871, 203
- Luo, A.-L., Zhao, Y.-H., Zhao, G., et al. 2015, *RAA (Research in Astronomy and Astrophysics)*, 15, 1095
- Maceroni, C., Milano, L., & Russo, G. 1982, *A&AS*, 49, 123
- McLean, B. J., & Hilditch, R. W. 1983, *MNRAS*, 203, 1
- Nelson, R. H. 2004, *Information Bulletin on Variable Stars*, 5493, 1
- Nelson, R. H. 2006, *Information Bulletin on Variable Stars*, 5672, 1
- Nelson, R. H. 2009, *Information Bulletin on Variable Stars*, 5875, 1
- Nelson, R. H. 2013, *Information Bulletin on Variable Stars*, 6050, 1
- Nelson, R. H. 2016, *Information Bulletin on Variable Stars*, 6164, 1
- Ogoza, W. 1995, *Information Bulletin on Variable Stars*, 4263, 1
- Ogloza, W. 1997, *Information Bulletin on Variable Stars*, 4534, 1
- Ogloza, W., Drozd, M., & Zola, S. 2000, *Information Bulletin on Variable Stars*, 4877, 1
- O'Connell, D. J. K. 1951, *MNRAS*, 111, 642
- Pagel, L. 2018, *Information Bulletin on Variable Stars*, 6244, 1
- Parimucha, S., Vanko, M., Pribulla, T., et al. 2007, *Information Bulletin on Variable Stars*, 5777, 1
- Parimucha, S., Dubovsky, P., Baludansky, D., et al. 2009, *Information Bulletin on Variable Stars*, 5898, 1
- Parimucha, S., Dubovsky, P., Vanko, M., et al. 2011, *Information Bulletin on Variable Stars*, 5980, 1
- Parimucha, S., Dubovsky, P., & Vanko, M. 2013, *Information Bulletin on Variable Stars*, 6044, 1
- Parimucha, S., Dubovsky, P., Kudak, V., et al. 2016, *Information Bulletin on Variable Stars*, 6167, 1
- Paschke, A. & Brat, L. 2006, *Open European Journal on Variable Stars*, 23, 13
- Pi, Q.F., Zhang, L.Y., Bi, S.L., et al. 2019, *ApJ*, 877, 75
- Press, W. H., Teukolsky, S. A., Vetterling, W. T., et al. 1992, *Numerical recipes in FORTRAN. The art of scientific computing*, Cambridge: University Press
- Pribulla, T., Baludansky, D., Chochol, D., et al. 2005, *Information Bulletin on Variable Stars*, 5668, 1
- Pribulla, T., Rucinski, S. M., Conidis, G., et al. 2007, *AJ*, 133, 1977
- Qian, S.-B., Zhang, J., Zhu, L.-Y., et al. 2012, *MNRAS*, 423, 3646
- Qian, S.-B., Li, K., Liao, W.-P., et al. 2013, *AJ*, 145, 91.
- Qian, Shengbang. 2001, *Ap&SS*, 278, 415
- Ruciński, S. M. 1973, *Acta Astronomica*, 23, 79
- Rucinski, S. M. 1976, *PASP*, 88, 777
- Safar, J., & Zejda, M. 2000, *Information Bulletin on Variable Stars*, 4888, 1
- Safar, J., & Zejda, M. 2002, *Information Bulletin on Variable Stars*, 5263, 1
- Şenavcı, H. V., Bahar, E., Montes, D., et al. 2018, *MNRAS*, 479, 875
- van Hamme, W. 1993, *AJ*, 106, 209
- Wilson, R. E. 1979, *ApJ*, 234, 1054
- Wilson, R. E. 1990, *ApJ*, 356, 613
- Wilson, R. E. 1994, *PASP*, 106, 921
- Wilson, R. E. 2008, *ApJ*, 672, 575
- Wilson, R. E., & Devinney, E. J. 1971, *ApJ*, 166, 605
- Wu, Y., Luo, A.-L., Li, H.-N., et al. 2011, *RAA (Research in Astronomy and Astrophysics)*, 11, 924
- Yang, Y.-G., Dai, J.-M., Yin, X.-G., et al. 2007, *AJ*, 134, 179
- Yang, Y.-G., Shao, Z.-Y., Pan, H.-J., et al. 2011, *PASP*, 123, 895
- Yang, Y., & Liu, Q. 2003, *PASP*, 115, 748
- Yang, Y.-G., Lü, G.-L., Yin, X.-G., et al. 2009, *AJ*, 137, 236
- Zhang, L. Y., Lu, H. P., Han, X. M., et al. 2018, *NewA*, 61, 36
- Zhang, L. Y., Long, L., Shi, J. R., et al. 2020, *MNRAS*, 495, 1252
- Zhukov, G. V. 1976, *Astronomicheskij Tsirkulyar* 918, 7
- Zhukov, G. V. 1983, *Information Bulletin on Variable Stars*, 2416, 1
- Zhukov, G. V. 1985, *Pisma v Astronomicheskii Zhurnal*, 11, 101
- Zhou, H.-N. 1988, *Ap&SS*, 141, 199
- Zhou, A.-Y., Jiang, X.-J., Zhang, Y.-P., et al. 2009, *RAA (Research in Astronomy and Astrophysics)*, 9, 349
- Zola, S., Gazeas, K., Kreiner, J. M., et al. 2010, *MNRAS*, 408, 464